Mon. Not. R. Astron. Soc. **389,** 949–954 (2008) doi:10.1111/j.1365-2966.2008.13616.x

Multicolour time series photometry of 2MASS 1207−3932

C. Koen★

Department of Statistics, University of the Western Cape, Private Bag X17, Bellville, 7535 Cape, South Africa

Accepted 2008 June 18. Received 2008 June 17; in original form 2008 April 30

ABSTRACT

Time series photometry in *VRI* of the young brown dwarf Two-Micron All-Sky Survey (2MASS) J1207334−393254 is presented. Variability in *I* is insignificant, but amplitudes up to ∼0.2 mag in *R*, and ∼0.55 mag in *V*, are seen within a single night. There is also microvariability on time-scales of an hour or so, which appears to be present in data from all the three filters. There may be a non-sinusoidal periodicity of about half a day in the *V* and *R* data. A likely explanation for the variability is the presence of accretion hot spots.

Key words: stars: individual: 2MASS J1207334−393254 – stars: low-mass, brown dwarfs – stars: spots – stars: variables: other.

1 INTRODUCTION

An extensive discussion on the properties of 2MASS J1207334−393254 (abbreviated as '2M 1207−3932') can be found in Mohanty et al. (2007). For convenience, some of the information is repeated here. The object is a young (age < 10 Myr) binary member of the TW Hydrae association. It consists of an M8 brown dwarf primary (2M 1207−3932a) and a companion (2M 1207−3932b) with an L spectral type. The structure of the system is complex – the primary is surrounded by a disc, which has both dust and hot gas components (see Riaz & Gizis 2007; Morrow et al. 2008; Riaz & Gizis 2008, for detailed discussions of the disc properties). The disc inclination is near to edge-on ($i \sim 60°$–$70°$). There may also be a disc associated with 2M 1207−3932b.

Several attempts have been made to estimate the distance to 2M 1207−3932. The results are summarized in Ducourant et al. (2008), who find a value of 52 ± 1 pc.

The similarity of accreting young brown dwarfs to classical T Tauri stars prompted efforts to detect radio (Osten & Jayawardhana 2006) and X-ray (Gizis & Bharat 2004) emission from 2M 1207−3932, but only upper limits could be set.

The system appears not to have been monitored photometrically, but reports of time series spectroscopy have been published by Scholz, Jayawardhana & Brandeker (2005b) and Stelzer, Scholz & Jayawardhana (2007). Scholz et al. (2005b) obtained one to three high-resolution spectra on nine nights, spread over two months. Substantial changes in the emission line spectrum were seen, particularly in Hα. According to the authors, the '. . .profile exhibits dramatic, quasi-periodic changes. . .over the course of a night'. Attention was first drawn to variable Hα profiles by Mohanty, Jayawardhana & Barrado y Navascués (2003).

Of particular interest is the presence of a redshifted absorption feature superimposed on the broad Hα emission profile. Amongst the T Tauri stars, those exhibiting this feature, believed to be a signature of infalling gas, are classified as YY Orionis stars. It appears that the Hα line in 2M 1207−3932 may be more variable than is usually seen in the YY Ori stars (e.g. Stahler & Palla 2004).

The same set of spectra was also analysed by Scholz & Jayawardhana (2006), who find evidence for a hot outflow (wind). This has since been confirmed by Whelan et al. (2007), who found a bipolar outflow from 2M 1207−3932. Scholz & Jayawardhana (2006) also make the point that '. . .most of the variability is produced on time-scales of a few weeks rather than days'.

The second monitoring campaign, by Stelzer et al. (2007), was more intensive, with 59 spectra obtained over two consecutive nights. Five additional spectra were also acquired during the preceding three months. All Hα emission lines were double; higher-order Balmer lines were also mostly double-peaked. The variability in strength and wavelength of the central absorption component of Hα are interpreted in terms of changes in aspect of an accretion hot spot. According to the authors, the variability was '. . .much less pronounced and systematic than expected from previous data'.

Stelzer et al. (2007) deduced accretion rates of around $10^{-10}\,M_{\odot}\,yr^{-1}$, and stated that the rate had varied by almost two orders of magnitude over the time that 2M 1207−3932 had been studied. Herczeg & Hillenbrand (2008) obtained low-resolution spectra extending into the blue and derived an accretion rate of $10^{-11.7}\,M_{\odot}\,yr^{-1}$ from the Balmer jump.

The first two photometric runs reported below fall within the period spanned by the Stelzer et al. (2007) study: the longer run precedes the high time resolution spectroscopy by two weeks. Interestingly, the level of variability in the first two sets of photometry was lower than in the later runs (obtained two years later) – recalling the remark by Stelzer et al. (2007) that the brown dwarf was not very active during the acquisition of their observations.

The resemblance of 2M 1207−3932 to classical T Tauri stars suggests that similar observational techniques could be applied to it. In particular, photometric monitoring, such as the campaign on AA Tau described by Bouvier et al. (2003), has been successful in

★E-mail: ckoen@uwc.ac.za

deducing a wealth of information about that star. The work described below suggests that the study of 2M 1207−3932 could likewise benefit from extensive photometric monitoring.

The experimental configuration used to obtain the photometry is described next, followed by a discussion of the light curves. Brief concluding remarks are made in Section 4.

Section 3.2 describes a frequency analysis of the time series data. A few words of explanation are added here, for the benefit of those readers who may be unfamiliar with the field. A standard tool used for analysing data containing possible periodicities is the periodogram, or power spectrum. In this paper, a variant, the 'amplitude spectrum' is used: as the name suggests, it is a scaled version of the spectrum that reflects the amplitude of variation at a given frequency, rather than the power. Amplitude spectra can be dominated by large-amplitude features, which may be of secondary interest, and which could obscure the presence of interesting periodicities. A common example is the large power excess at low frequencies due to slow, possibly aperiodic, drifts in the mean brightness level of a star. A useful device for dealing with this is 'pre-whitening': fitting a low-frequency sinusoid to the data, subtracting it and proceeding with the residuals. The presence of lower amplitude periodicities will be much clearer in the pre-whitened data.

2 THE OBSERVATIONS

All measurements were made with the South African Astronomical Observatory (SAAO) CCD camera mounted on the SAAO 1.9-m telescope at Sutherland, South Africa. The camera, which has a field of view of about 2.5×2.5 arcmin^2, was operated in 2×2 prebinning mode, which gave a reasonable readout time of 20 s. The effective pixel scale was 0.24 arcsec pixel^{-1}, which was adequate for typical seeing conditions (1–3 arcsec). Exposure times were tailored to the various filters used, and to prevailing atmospheric conditions. Photometric reductions were performed using an automated version of DOPHOT (Schechter, Mateo & Saha 1993).

Short observing runs were made on 2006 March 28 and April 27/28. More extended sets of measurements were obtained on three successive nights over the interval 2008 March 30 to April 2. A log of the observations is given in Table 1. Cousins R_C and I_C filters were used throughout, but will be conveniently referred to as R and I below.

Light curves can be seen in Figs 1–3. All measurements have been differentially corrected, using five to 10 comparison stars in the field of view. The brightest of these (DENIS J120731.0−393228) was used to set the nightly zero-points; the values $I = 13.477, R = 14.17, V = 14.30$ were taken from the DENIS and NOMAD (Naval Observatory Merged Astrometric Data set) catalogues (see Epchtein et al. 1999; Zacharias et al. 2004, respectively). The magnitudes in

Table 1. The observing log: $T_{\rm int}$ is the exposure time and N the minimum number of useful measurements through any filter obtained during the run. All runs were continuous, expect for that on JD 245 4558, which suffered an interruption due to cloudy weather.

Starting time (HJD 245 0000+)	Filters	$T_{\rm int}$ (s)	Run length (h)	N
3823.3232	*RI*	90, 60	4.3	79
3853.2239	*VRI*	120–150, 90, 50	6.2	63
4556.2506	*VRI*	150–200, 90–120, 60	9.3	72
4557.2391	*VRIZ*	180–200, 120, 60, 60	9.4	54
4558.2617	*VRI*	150–180, 100–120, 60	8.8	57

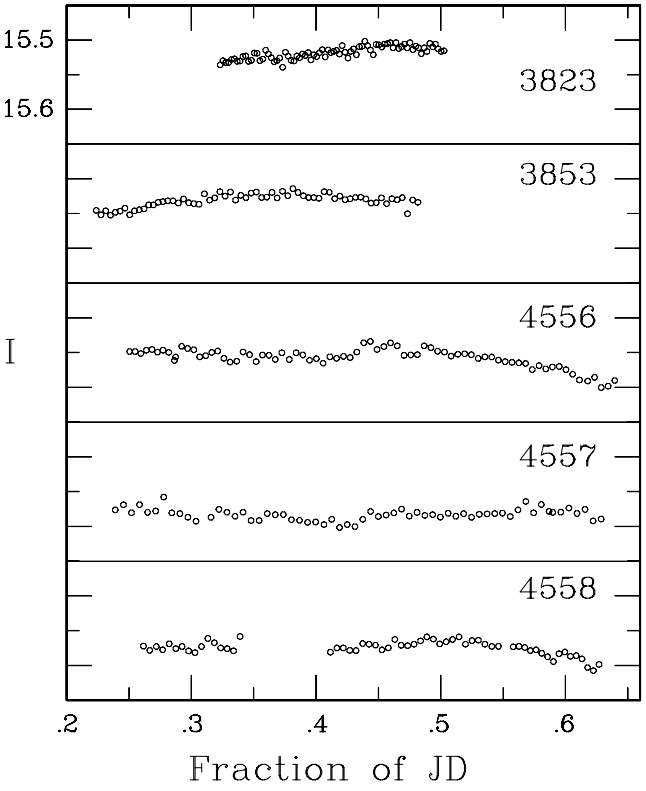

Figure 1. Light curves obtained through the I_C filter. The scale is the same on each of the panels in the diagram. Panels are labelled with the last four digits of the Julian Day of observation.

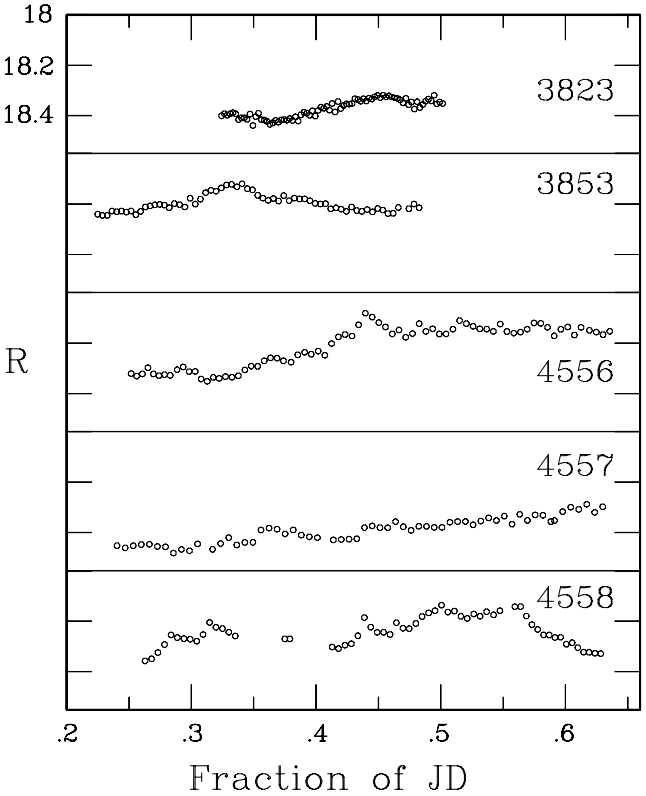

Figure 2. Light curves obtained though the R_C filter. The scale is the same on each of the panels in the diagram. Panels are labelled with the last four digits of the Julian Day of observation.

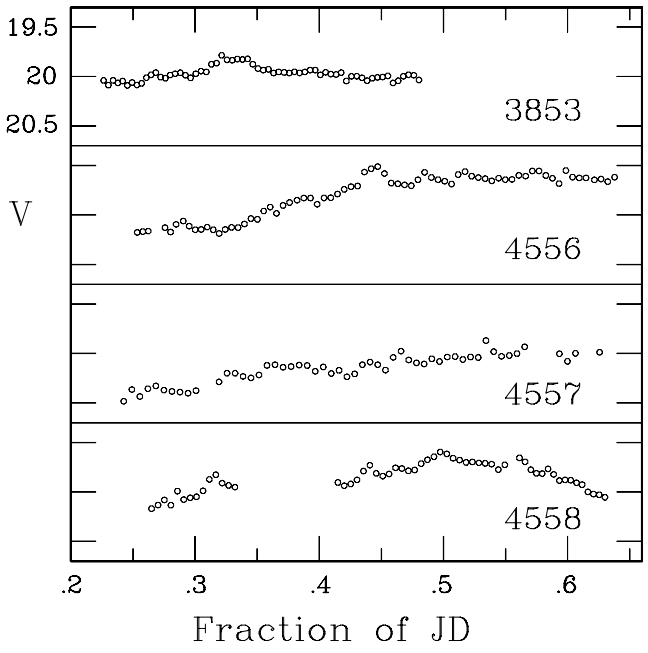

Figure 3. Light curves obtained though the *V* filter. The scale is the same on each of the panels in the diagram. Panels are labelled with the last four digits of the Julian Day of observation.

the plots can be compared with the measurements $V = 20.15, R = 18.08$ and $I = 15.95$ given by Ducourant et al. (2008): the mean *R* and *I* magnitudes measured at SAAO are, respectively, about 0.3 mag fainter, and 0.4 mag brighter, while the mean *V* is quite similar to the Ducourant et al. (2008) value. Photometric errors of 0.17 in *R*, and 0.13 in *I*, are quoted by Ducourant et al. (2008), so that these differences are acceptable, given the crude standardization of the SAAO data.

A quantitative measure of the data quality is given by the measurement scatter (standard deviation) of constant stars of similar brightness to 2M 1207−3932. The numbers of apparently constant stars with magnitudes within 0.5 mag of 2M 1207−3932 were 3, 4, 3 and 2 in *I*, *R*, *V* and *Z*, respectively. The nightly scatter in the measurements of these stars was in the ranges 0.004–0.009, 0.006–0.019, 0.019–0.028 and 0.006–0.012 mag, respectively.

Since the secondary of the system was undetectable with the exposure times used, all measurements refer to 2M1207−3932a only.

3 DISCUSSION OF THE LIGHT CURVES

Examination of the plots shows that the level of variability increases towards the blue. There is little evidence of brightness changes in *I* and *Z* (not shown), whereas the *V* magnitude can change by several tenths of a magnitude over a few hours. The level of variability is not always the same – the object appears to have been rather less active during the first two runs. There are also some fairly rapid (time-scales of the order of an hour) small systematic brightness changes superimposed on the large *V* and *R* variations measured on HJD 245 4556 and 245 4558. Note that some of these microvariations also seem to be present in the *I* band (see the interval HJD 245 4556.4-245 4556.5). Amplitudes of the microvariations are roughly of the order of 0.15, 0.06 and 0.03 mag in *V, R* and *I*, respectively.

Table 2. Rough estimates of the amplitudes of variability seen during extended runs on 2M 1207−3932 (Columns 2 and 3); estimates of the hot-spot temperature and the filling factor (Columns 3 and4) and the *I*-band amplitude implied by $T_{\rm spot}$ (last column).

Date (HJD 245 0000+)	A_R (mag)	A_V (mag)	$T_{\rm spot}$ (K)	Filling factor *f*	ΔI (mag)
3853	0.12	0.22	4060	5E-3	0.07
4556	0.20	0.55	8800	4E-4	0.07
4557	0.15	0.40	7420	5E-4	0.06
4558	0.15	0.40	7420	5E-4	0.06

3.1 Accretion hot spots

Irregular photometric variations have been observed in other young brown dwarfs by Scholz & Eislöffel (2004, 2005). The brightness changes are ascribed to a combination of accretion, which gives rise to hot spots, and rotation. The accretion hot spots may be quite variable and/or short lived. Furthermore, as pointed out by, for example, Scholz, Eislöffel & Froebrich (2005a), the steep rise in amplitude with decreasing wavelength implies the presence of bright spots on the surface (rather than dark spots).

It is noteworthy though that the *I*-band variations of typically several tenths of a magnitude observed by Scholz & Eislöffel (2004, 2005) are much larger than those seen in 2M 1207−3932. It is also interesting that the *I*-band light curves in Fig. 1 may be rather different from those in the shorter wavelengths (Figs 2 and 3).

The extent of the brightness changes (i.e. the differences between maximum and minimum) in the *V* and *R* bands was measured from the light curves and is given in Table 2. Following the blackbody assumption applied to T Tauri spots in Stahler & Palla (2004)

$$\Delta m_\lambda = -2.5 \log_{10} \left\{ 1 - f \left[1 - \frac{B_\lambda(T_{\rm spot})}{B_\lambda(T_{\rm star})} \right] \right\}, \quad (1)$$

where $B_\lambda(T)$ is the Planck function at wavelength λ and temperature *T*. The 'filling factor' *f* is the fraction of the stellar hemisphere covered by the spot. Writing equation (1) for both the *V* (λ = 5500 Å) and *R* (λ = 6600 Å) data, two simultaneous equations for *f* and $T_{\rm spot}$ are obtained. These can be further manipulated to give a single equation for $T_{\rm spot}$, which can be solved numerically. The solutions are also given in Table 2, where $T_{\rm star} = 2550$ K has been adopted from Mohanty et al. (2007).

The filling factors in Table 2 (ranging from 4×10^{-4} to 5×10^{-3}) appear to be unrealistically small. These follow because the substantial *differences* between Δm_V and Δm_R require high temperatures for $T_{\rm spot}$ (∼4000–9000 K); such high spot temperatures would, however, give rise to very large flux changes unless *f* were quite small. One possible explanation of the small solutions for *f* is that a substantial part of the hot-spot flux at shorter wavelengths is in the form of emission lines, rather than continuum radiation. The paucity of strong emission lines falling in the *I* band would then explain the relatively low variability amplitude in that bandpass. Of course, the blackbody assumption is also unrealistic. On the positive side, similar spot temperatures (6500–7500 K) were obtained by Herczeg & Hillenbrand (2008) from spectra extending beyond the Balmer jump to 3000 Å.

Table 2 also shows predicted changes in the *I* band, based on the solutions for $T_{\rm spot}$ and *f*. These are somewhat larger than the observed changes (which are typically of the order of 0.04 mag or so; see Fig. 1).

3.2 Are there periodicities in the data?

In their observations of irregularly varying young brown dwarfs, Scholz & Eislöffel (2004, 2005) found that there were underlying periodicities in some of the light curves. This point is therefore worth investigating in the case of the present data. The fact that $v \sin i = 13$ km s^{-1} (Mohanty et al. 2003) implies an upper limit to the rotation period of about 25 h (Scholz et al. 2005b). Therefore, any periodicity – if it is due to rotation – needs to be about a day, or shorter. Scholz et al. (2005b) and Stelzer et al. (2007) do find variability on this time-scale in their data. If the rotation period is of the order of a day, then it would mean that accretion on to only one of the magnetic poles of 2M 1207−3932a is observed. Given the almost edge-on orientation of the circum-object disc (e.g. Whelan et al. 2007), it is possible that both poles could be observable. In that case, a rotation period of one day could lead to an observed period of half a day. To the author's eye, the inspection of Figs 2 and 3 does suggest substantial variability on a time-scale of a few hours.

There is a gap of about two years between the first two photometric runs and the last three, so only the latter are taken into account in what follows. Unfortunately, there is no unambiguous period: the value(s) depends on the assumptions made. Some plausible possibilities are: (i) take data for all three nights into account, in the form in which it appears in Figs 2 and 3, and fit a sinusoid; (ii) assume that there is a slow drift in the mean level, and fit individual levels for each night as well as an underlying sinusoid and (iii) assume that the variation is not necessarily sinusoidal.

Model (i) above seems the simplest, but essentially reduces to a variation of (ii), since the differences in nightly means require modelling by low-frequency sinusoids. Frequencies of 0.518 and 0.528 d^{-1} are obtained for *R* and *V* data, respectively; after pre-whitening by these, best-fitting frequencies of 2.003 and 2.035 d^{-1} (amplitudes 0.061 and 0.195 mag) follow. Least-squares fits to the pre-whitened data of these sinusoids are plotted in Figs 4 and 5.

Of course, it seems more realistic to assume that the same frequencies are present in the *R* and *V* data. However, the intention here is to explore the similarity/difference of the results obtained from the two data sets, rather than to arrive at a definitive description which encompasses all the data.

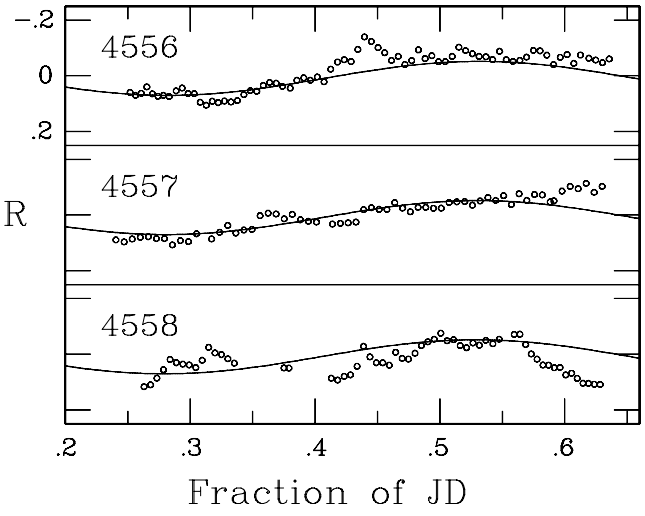

Figure 4. A fit to *R*-band data of a sinusoid with a period of 0.499 d. The observations have first been pre-whitened by subtraction of a low-frequency ($f = 0.518$ d^{-1}) sinusoid.

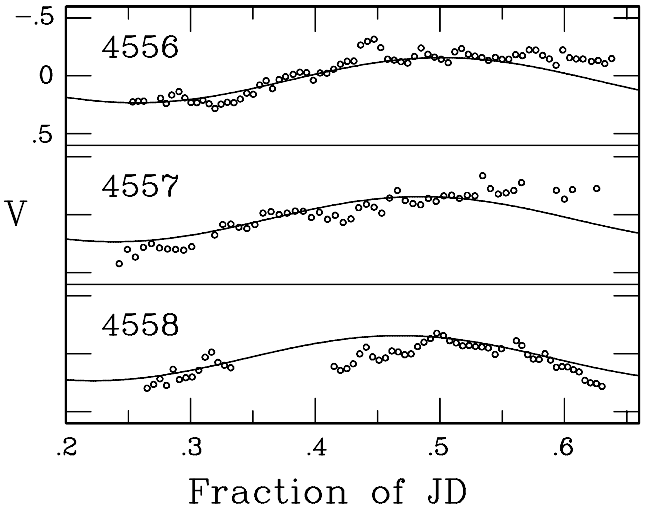

Figure 5. A fit to *V*-band data of a sinusoid with a period of 0.491 d. The observations have first been pre-whitened by subtraction of a low-frequency ($f = 0.528$ d^{-1}) sinusoid.

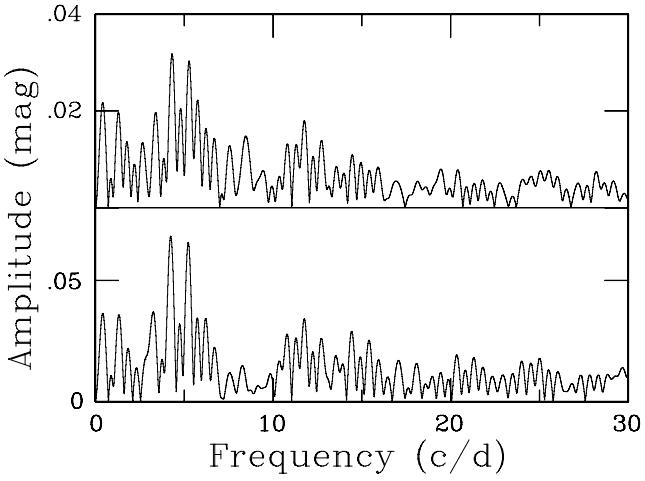

Figure 6. Amplitude spectra of the *R* (top panel) and *V* (bottom panel) residuals, after pre-whitening each by two low frequencies and a ∼2 d^{-1} sinusoid. (In the case of the *R* band, the pre-whitening is with frequencies 0.518, 0.722 and 2.003 d^{-1}; for the *V*-band 0.528, 0.741 and 2.035 d^{-1}.)

Considerable power remains in the amplitude spectra after also pre-whitening the *R* and *V* data by the ∼2 d^{-1} variations. After pre-whitening by a further low-frequency component (frequencies of 0.733 and 0.741 d^{-1} for *R* and *V*, respectively), the amplitude spectra in Fig. 6 result. The maxima are at frequencies 4.323 (*R*) and 4.245 d^{-1} (*V*); fitted sinusoids have amplitudes of 0.031 and 0.067 mag, respectively. Fig. 7 shows the data (pre-whitened by the three lower frequencies) folded with respect to these frequencies.

The formal errors of the ∼2 d^{-1} frequencies are of the order of 0.01–0.02. A glance at the relevant amplitude spectral peaks in Fig. 8 shows that these are probably severe underestimates. Similar considerations apply to the ∼4.3 d^{-1} frequencies. It is therefore quite conceivable that the 4.2–4.3 d^{-1} frequencies are in fact the first harmonics of the ∼2 d^{-1} frequencies, i.e. the variations are of double-wave, rather than sinusoidal, form.

In view of these results, a combination of models (ii) and (iii) seems appropriate. Denoting the magnitude measured at time *t*

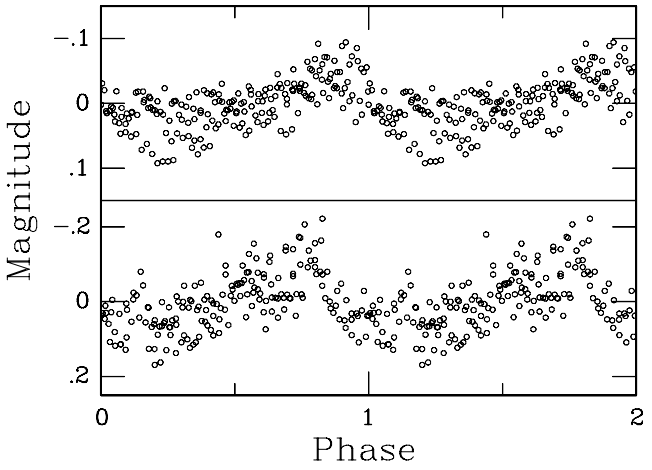

Figure 7. The *R* (top panel) and *V* (bottom panel) residuals (data after the removal of three frequencies each; see Fig. 6 caption), folded with respect to frequencies 4.323 d^{-1} (*R*) and 4.245 d^{-1} (*I*). These frequencies are the two best-fitting values from the amplitude spectra in Fig. 6.

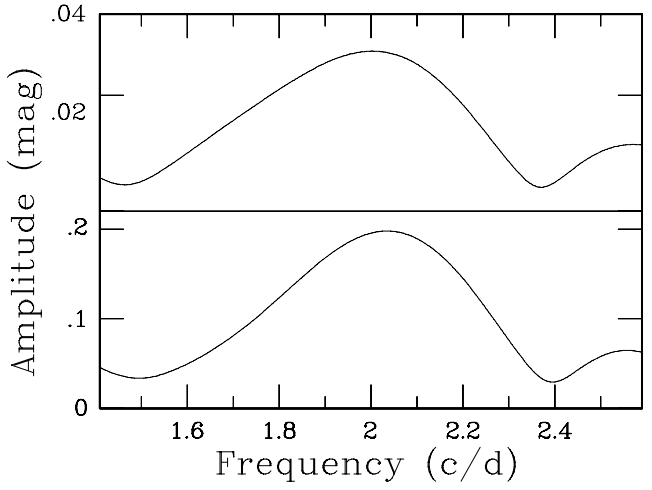

Figure 8. Detail of the highest peak in the amplitude spectra after the removal of a single low frequency. Top panel: *R* ($F = 0.518$ d^{-1} pre-whitened); bottom panel: *V* ($F = 0.528$ d^{1} pre-whitened).

during night *k* by $y_k(t)$,

$$y_k(t) = \mu_k + A_1 \cos(2\pi f t + \phi_1) + A_1 \cos(4\pi f t + \phi_1) + \text{error} \quad k = 1, 2, 3, \tag{2}$$

where *f* is the frequency; A_1 and A_2 are amplitudes; ϕ_1 and ϕ_2 are phases and μ_k is mean level of the light curve during night *k*. Fitting of this model by least squares is discussed by Koen (2003). Fig. 9 shows 'least-squares spectra' for the *R* and *V* data; the quantity on the vertical axis is the log of the residual sum of squares, i.e. the best-fitting frequency is given by the point where it reaches a minimum. The solutions are given in Table 3: the best-fitting frequencies are 2.104 and 2.086 d^{-1} for *R* and *I*, respectively.

Although a lot more could be said about models of the light curves in Figs 2 and 3, there seems to be little point, given the uncertainties involved.

The *I*-band light curves in Fig. 1 are now briefly considered. The amplitude spectrum is again dominated by a long period component, with frequency similar (0.59 d^{-1}) to that found in the *R* and *V* data. If this is pre-whitened from the data, the spectrum maximum is at 2.41 d^{-1} (amplitude 0.008 mag). Pre-whitening again, $f = 4.006$ d^{-1} (amplitude 0.008 mag) is obtained – similar to the proposed harmonic frequency in the *R* and *V* data, but also suspiciously close to an integer multiple of one day. The different stages of pre-whitening are illustrated in Fig. 10.

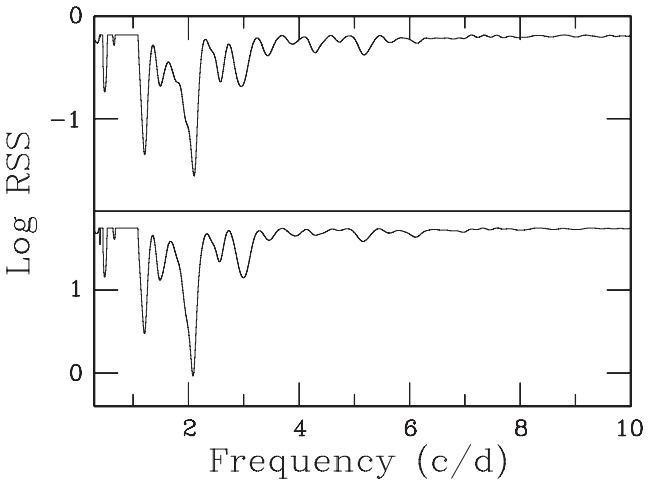

Figure 9. Least-squares spectra, allowing for nightly zero-point shifts, of the raw *R* (top panel) and *V* (bottom panel) data (see Koen 2003 for details).

Table 3. Least-squares parameter estimates for the model of equation (2) fitted to the raw data. The μ_k are nightly zero-points; *f* is the frequency in d^{-1} ; A_1 and A_2 are amplitudes of the fundamental and first harmonic components; and ϕ_1 and ϕ_2 are the phases of the fundamental and first harmonics.

	R band	
$\mu_1 = 18.21$	$\mu_2 = 18.40$	$\mu_3 = 18.26$
$f = 2.104$	$A_1 = 0.070$	$\phi_1 = -1.92$
	$A_2 = 0.029$	$\phi_2 = -3.00$
	V band	
$\mu_1 = 19.80$	$\mu_2 = 20.18$	$\mu_3 = 19.91$
$f = 2.086$	$A_1 = 0.213$	$\phi_1 = -1.01$
	$A_2 = 0.042$	$\phi_2 = -1.50$

4 CONCLUSIONS

New aspects of variability in 2M 1207−3932 revealed by the photometry are as follows.

(i) Amplitudes in the *Z* and *I* bands are very small, rising sharply with decreasing wavelength in *R* and *V*.

(ii) The *R* and *V* data show both large, slow changes and smaller amplitude changes on time-scales of an hour or so.

(iii) Large amplitude variability patterns in *R* and *V* are not mimicked by changes in *I* and *Z* [see also point (v) below], but similar microvariability is seen in *VRI*.

(iv) The steep increase in amplitude with decreasing wavelength implies high blackbody temperatures and very low filling factors, if a 'hot-spot' accretion model is adopted.

(v) The currently available data favour a non-sinusoidal periodicity in *R* and *V*, with a frequency of about 2.1 d^{-1}, which is subject to nightly changes in mean level. A reasonable explanation, consistent with the expected rotation period close to a day, is the presence of two accretion hot spots, both of which are visible.

(vi) This periodicity could not be identified in the *I*-band data.

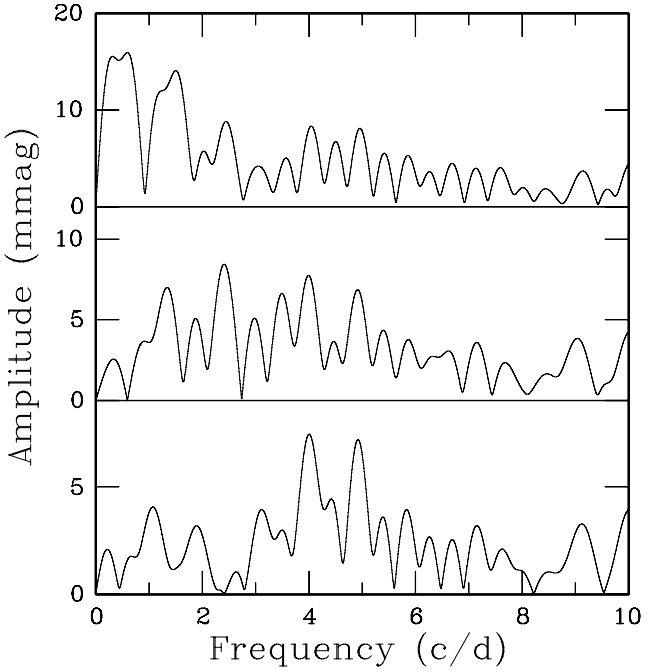

Figure 10. Amplitude spectra of the *I*-band data. Top panel: spectrum of the raw data. Middle panel: spectrum of the residuals after pre-whitening by the most prominent frequency in the top panel. Bottom panel: spectrum of the residuals after pre-whitening by the two most prominent frequencies. Note that the vertical scale in the top panel is different from those in the other two panels, and that magnitudes are in millimag.

It is clear that photometric monitoring in several passbands can supply information which complements spectroscopic time series. Furthermore, photometry has the advantage of fine time resolution, even with a modest-sized telescope (the bulk of the Stelzer et al. 2007 observations were made with the ESO VLT 2). It is also clear that a considerable amount of data may be required in order to arrive at a reliable model for the variability in 2M 1207−3932.

ACKNOWLEDGMENTS

Telescope time allocation by SAAO, and data taken from the DENIS and NOMAD catalogues, is gratefully acknowledged. Conversations with Professor David Kilkenny (SAAO and University of the Western Cape) were very useful. The author also thanks Dr Alexander Scholz (University of St Andrews) for kindly supplying a number of relevant references.

REFERENCES

Bouvier J. et al., 2003, A&A, 409, 169
Ducourant C., Teixeira R., Chauvin G., Daigne G., Le Campion J.-F., Song I., Zuckerman B., 2008, A&A, 477, L1
Epchtein N. et al., 1999, A&A, 349, 236
Gizis J. E., Bharat R., 2004, ApJ, 608, L113
Herczeg G. J., Hillenbrand L. A., 2008, ApJ, 681, 594
Koen C., 2003, MNRAS, 346, 473
Mohanty S., Jayawardhana R., Barrado y Navascués D., 2003, ApJ, 593, L109
Mohanty S., Jayawardhana R., Huélamo N., Mamajek E., 2007, ApJ, 657, 1064
Morrow A. L. et al., 2008, ApJ, 676, L143
Osten R. A., Jayawardhana R., 2006, ApJ, 644, L67
Riaz B., Gizis J. E., 2007, ApJ, 661, 354
Riaz B., Gizis J. E., 2008, ApJ, 681, 1584
Schechter P. L., Mateo M., Saha A., 1993, PASP, 105, 1342
Scholz A., Eislöffel J., 2004, A&A, 419, 249
Scholz A., Eislöffel J., 2005, A&A, 429, 1007
Scholz A., Jayawardhana R., 2006, ApJ, 638, 1056
Scholz A., Eislöffel J., Froebrich D., 2005a, A&A, 438, 675
Scholz A., Jayawardhana R., Brandeker A., 2005b, ApJ, 629, L41
Stahler S. W., Palla F., 2004, The Formation of Stars. Wiley-VCH, Weinheim
Stelzer B., Scholz A., Jayawardhana R., 2007, ApJ, 671, 842
Whelan E. T., Ray T. P., Randich S., Bacciotti F., Jayawardhana R., Test L., Natta A., Mohanty S., 2007, ApJ, 659, L45
Zacharias N., Monet D. G., Levine S. E., Urban S. E., 2004, A&AS, 205, 4815

This paper has been typeset from a TEX/LATEX file prepared by the author.